



Herbert Wertheim
College of Engineering
UNIVERSITY of FLORIDA

Development of Age-Dependent Computational Phantoms

Wesley Bolch, University of Florida

Member, ICRP Committee 2

Chair, TG 96 – Computational Phantoms and Radiation Transport

Presentation Objectives

- 1. Review current work flow of ICRP Committee 2 and its Task Groups**
 - A. Dose coefficients for adults
 - B. Dose coefficients for infants, children, and adolescents

- 2. Review the historical lineage of models that have become the ICRP pediatric phantom series**

- 3. Review specific dosimetry models associated with these pediatric phantoms**
 - A. Blood distribution model
 - B. Skeletal tissue model
 - C. SAFs for internally emitted radiations

- 4. Review the development and two specific applications of a derived pediatric phantom library**
 - A. Radiation epidemiology of the medical imaging of children
 - B. Radiation epidemiology of the Japanese atomic bomb survivors

Following the development of the ICRP Publication 110 Reference Adult Phantoms, ICRP Committee 2 has developed, and continues to develop, dose coefficients for use in the radiological protection community:

External Exposures

ICRP Publication 116 - Provides DCs for occupational external exposures (2010)

Internal Exposures – The Occupational Intakes of Radionuclides (OIR) Series

ICRP Publication 130 – OIR Part 1 – Supporting Framework (2015)

ICRP Publication 133 – Supporting SAFs for the reference adults (2016)

ICRP Publication 134 – OIR Part 2 (2016)

ICRP Publication 137 – OIR Part 3 (2017)

OIR Part 2 – ICRP Publication 134

Hydrogen (H), Carbon (C), Phosphorus (P), Sulphur (S), Calcium (Ca), Iron (Fe), Cobalt (Co), Zinc (Zn), Strontium (Sr), Yttrium (Y), Zirconium (Zr), Niobium (Nb), Molybdenum (Mo) and Technetium (Tc).

OIR Part 3 – ICRP Publication 137

Ruthenium (Ru), Antimony (Sb), Tellurium (Te), Iodine (I), Caesium (Cs), Barium (Ba), Iridium (Ir), Lead (Pb), Bismuth (Bi), Polonium (Po), Radon (Rn), Radium (Ra), Thorium (Th) and Uranium (U).

OIR Part 4

Lanthanides series, actinium (Ac), protactinium (Pa) and transuranic elements

OIR Part 5

Fluorine (F), Sodium (Na), Magnesium (Mg), Potassium (K), Manganese (Mn), Nickel (Ni), Selenium (Se), Molybdenum (Mo), Technetium (Tc) and Silver (Ag) and most of the others

Other needed guidance for both external and internal dose coefficients involves exposures to members of the general public

External Exposures

ICRP C2 Task Group 90 – To provide DCs for environmental sources of radionuclides

Internal Exposures – The Environmental Intakes of Radionuclides (EIR) Series

ICRP C2 Task Group 95

EIR Part 1 – Every element currently described in OIR P2 to P4 plus Ag, Ni, and Se

EIR Part 2 – Remaining elements

EIR Part 3 – Breast-feeding infant internal dose coefficients for maternal intakes

EIR Part 4 – In utero internal dose coefficients for maternal intakes

Computational Phantoms of the non-Adult ICPR Reference Individuals

ICRP C2 Task Group 96 – To provide reference phantoms and SAFs for internally emitted photons, electrons, and alpha particles

Presentation Objectives

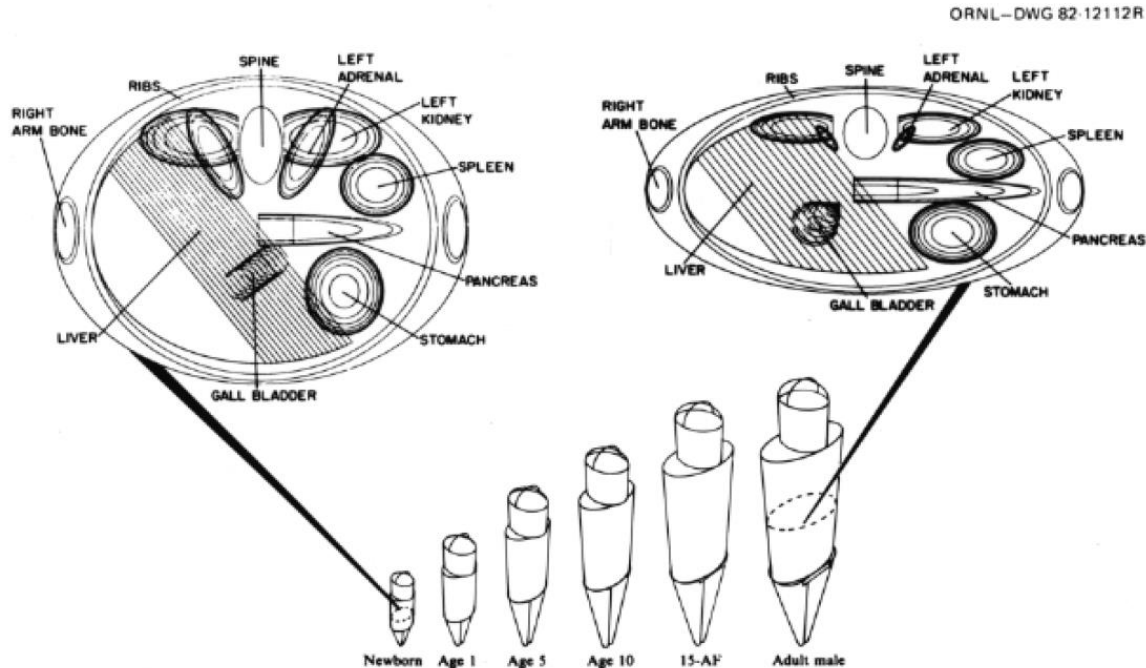
- 1. Review current work flow of ICRP Committee 2 and its Task Groups**
 - A. Dose coefficients for adult phantoms
 - B. Dose coefficients for pediatric phantoms
- 2. Review the historical lineage of models that have become the ICRP pediatric phantom series**
- 3. Review specific dosimetry models associated with these pediatric phantoms**
 - A. Blood distribution
 - B. Skeletal tissue models
 - C. SAFs for internally emitted radiations
- 4. Review the development and two specific applications of a derived pediatric phantom library**
 - A. Radiation epidemiology of the medical imaging of children
 - B. Radiation epidemiology of the Japanese atomic bomb survivors

ICRP Publication 89 defines 10 pediatric reference individuals with the following total body characteristics

Table 2.9. Reference values for height, mass, and surface area of the total body (Sections 4.2.1 and 4.2.2)

Age	Height (cm)		Mass (kg)		Surface area (m ²)	
	Male	Female	Male	Female	Male	Female
Newborn	51	51	3.5	3.5	0.24	0.24
1 year	76	76	10	10	0.48	0.48
5 years	109	109	19	19	0.78	0.78
10 years	138	138	32	32	1.12	1.12
15 years	167	161	56	53	1.62	1.55
Adult	176	163	73	60	1.90	1.66

Age-dependent dose coefficients in the past, based upon ICRP 26 and ICRP 60 radiation and tissue weighting factors, have employed organ doses computed using the ORNL stylized series of pediatric computational phantoms.



Origins of the new ICRP Pediatric Reference Phantoms

- *UF newborn voxel phantom*
- *UF Series A pediatric voxel phantoms*
- *UF Series B pediatric voxel phantoms*
- *UF/NCI series of hybrid-NURBS and hybrid-voxel reference phantoms*
- *Subsequent revisions to the UF/NCI series within TG 96*

Release of new ICRP Pediatric Reference Phantoms

- *ICRP Publication on pediatric phantoms – expected Fall 2018*
- *ICRP Publication on pediatric SAFs – expected Spring 2019*
(with internal ICRP use in Spring/Summer 2018)

UF Newborn Voxel Phantom

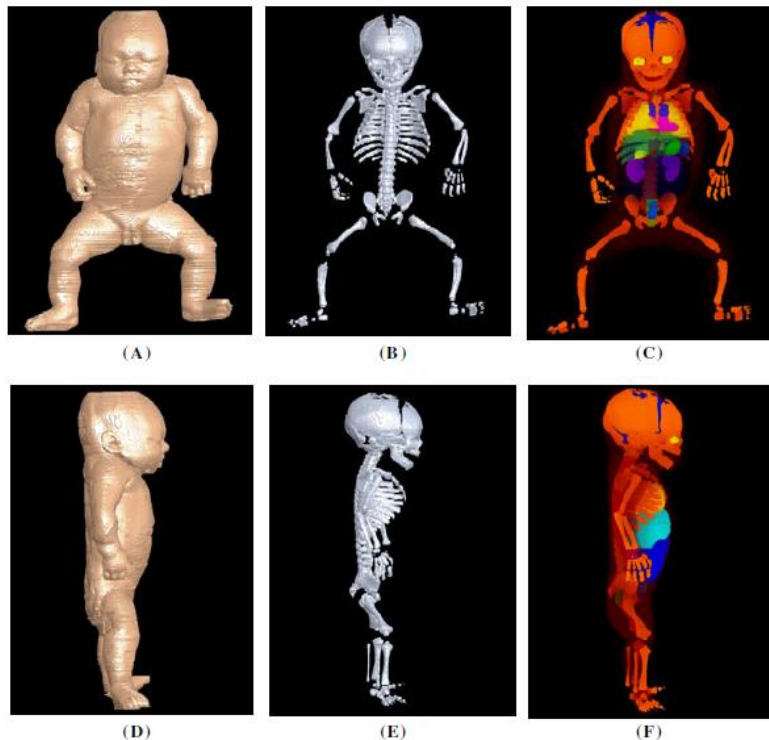


Figure 1. Frontal (top row) and right lateral (bottom row) views of the UF newborn tomographic model. Shown are the external skin (A and D), skeleton (B and E) and internal organs (C and F). In panel C, the liver and intestines have been removed for viewing the kidneys and other abdominal organs. These organs are shown in the right lateral view (panel F).

Phys. Med. Biol. 47 (2002) 3143–3164

Creation of two tomographic voxel models of paediatric patients in the first year of life

J C Nipper¹, J L Williams² and W E Bolch^{1,3}

¹ Biomedical Engineering Program, University of Florida, Gainesville, FL 32611-8300, USA

² Department of Radiology, University of Florida, Gainesville, FL 32611-8300, USA

³ Department of Nuclear and Radiological Engineering, University of Florida, Gainesville, FL 32611-8300, USA

Segmentation of a whole-body CT of a 6-day newborn female following unsuccessful cardiac surgery (512 x 512 x 485 array)

UF Series A Voxel Phantoms

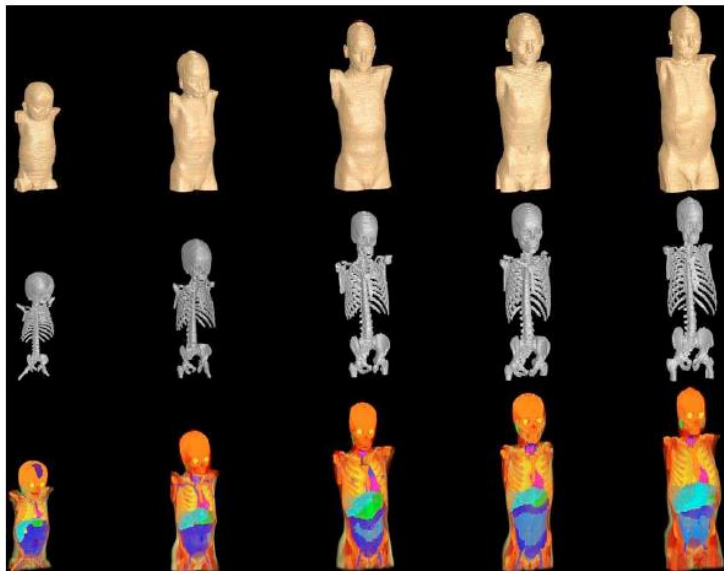


FIG. 2. Frontal views of the UF series of pediatric computational phantoms. Each of the three rows gives views of the phantom exterior, the skeletal system, and the internal organ structure, respectively. Image columns correspond to the 9-mo male, the 4-year female, the 8-year female, the 11-year male, and the 14-year male, respectively.

Med. Phys. 32 (12), December 2005

The UF series of tomographic computational phantoms of pediatric patients

Choonik Lee

Department of Nuclear and Radiological Engineering, University of Florida, Gainesville, Florida 32611

Jonathan L. Williams

Department of Radiology, University of Florida, Gainesville, Florida 32610

Choonsik Lee

Department of Nuclear and Radiological Engineering, University of Florida, Gainesville, Florida 32611

Wesley E. Bolch^{a)}

Departments of Nuclear and Radiological and Biomedical Engineering, University of Florida, Gainesville, Florida 32611

TABLE I. Computed tomography image sources for the development of the UF pediatric phantom series.

Phantom	Gender	Image source		Fused body image	
		Head series	CAP series	Voxel dimensions (mm)	Array size
UF 9 month	M	9 month male patient		$0.43 \times 0.43 \times 3.00$	$512 \times 512 \times 156$
UF 4 year	F	4 year female patient		$0.45 \times 0.45 \times 5.00$	$512 \times 512 \times 120$
UF 8 year	F	8 year female patient	8 year female patient	$0.58 \times 0.58 \times 6.00$	$512 \times 512 \times 121$
UF 11 year	M	12 year male patient	11 year male patient	$0.47 \times 0.47 \times 6.00$	$512 \times 512 \times 125$
UF 14 year	M	14 year male patient	14 year male patient	$0.625 \times 0.625 \times 6.00$	$512 \times 512 \times 133$

UF Series B Voxel Phantoms

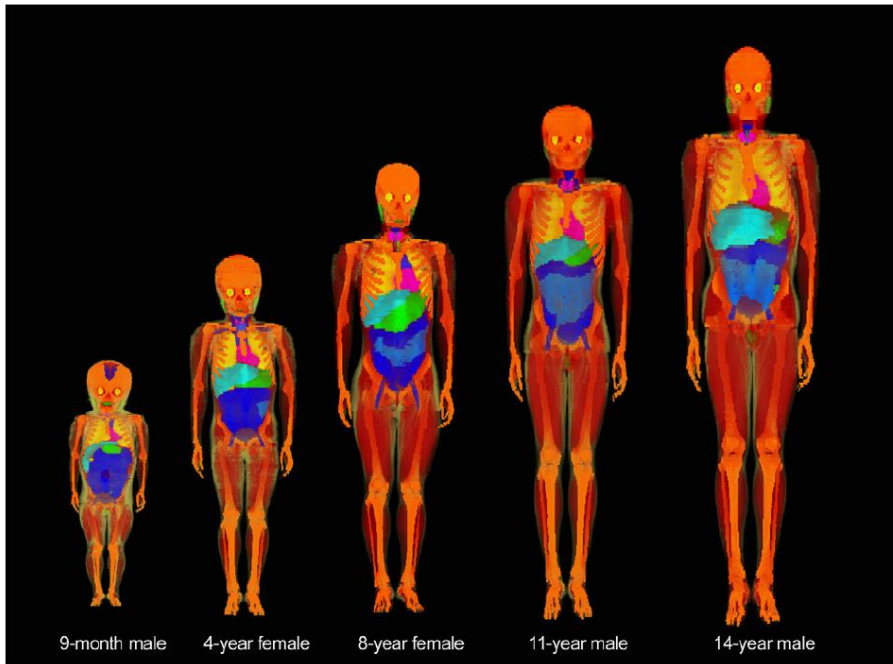


Figure 2. Frontal views of the UF Series B of paediatric computational phantoms. The phantoms include the 9-month male, the 4-year female, the 8-year female, the 11-year male and the 14-year male, respectively, from left to right. The phantom images are shown in a uniform relative scale across the phantom ages.

Phys. Med. Biol. **51** (2006) 4649–4661

Whole-body voxel phantoms of paediatric patients—UF Series B

Choonik Lee¹, Choonsik Lee¹, Jonathan L Williams²
and Wesley E Bolch^{1,3}

¹ Department of Nuclear and Radiological Engineering, University of Florida, Gainesville, FL 32611, USA

² Department of Radiology, University of Florida, Gainesville, FL 32610, USA

³ Department of Biomedical Engineering, University of Florida, Gainesville, FL 32611, USA

Table 1. Computed tomography image sources for the development of the UF Series B paediatric phantoms.

Phantom	Gender	Image sources			Fused body image	
		Head series	CAP series	Arms and legs	Voxel dimensions (mm)	Array size
UF 9-month	M	9-month male patient			0.86 × 0.86 × 3.00	289 × 180 × 241
UF 4-year	F	4-year female patient			0.90 × 0.90 × 5.00	351 × 207 × 211
UF 8-year	F	8-year female patient	8-year female patient	Adult volunteer	1.16 × 1.16 × 6.00	322 × 171 × 220
UF 11-year	M	12-year male patient	11-year male patient		0.94 × 0.94 × 6.00	398 × 242 × 252
UF 14-year	M	14-year male patient	14-year male patient		1.18 × 1.18 × 6.72	349 × 193 × 252

UF/NCI Family of Hybrid Phantoms

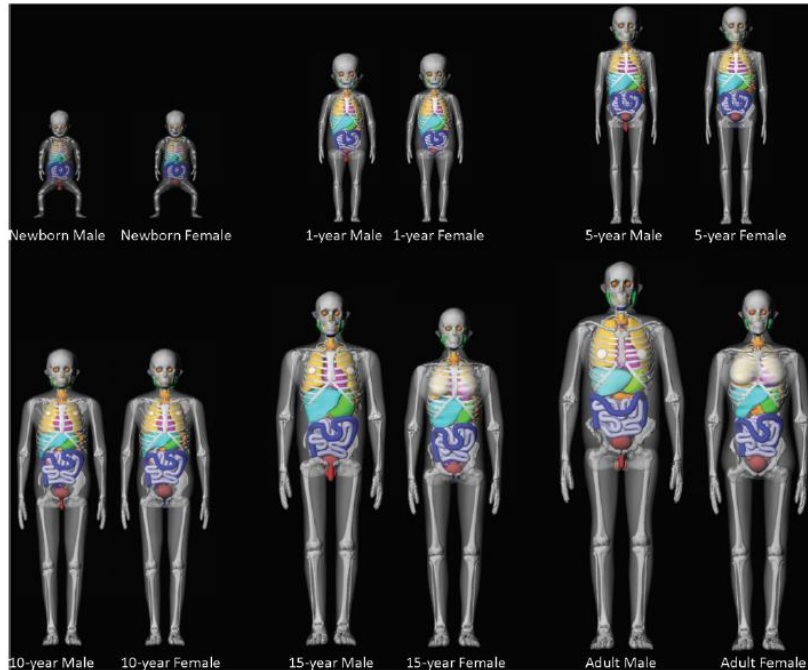


Figure 7. 3D frontal views of the entire series of UF hybrid pediatric and adult phantoms. The body contours were made semi-transparent for better viewing of internal anatomy.

Phys. Med. Biol. 55 (2010) 339–363

The UF family of reference hybrid phantoms for computational radiation dosimetry

Choonsik Lee¹, Daniel Lodwick², Jorge Hurtado², Deanna Pafundi², Jonathan L Williams³ and Wesley E Bolch^{4,5}

Table 1. CT image sources employed in the development of the UF hybrid phantom series.

	Head	Torso	C-Vertebrae	Arms and legs
UFH00MF			6 day F $0.586 \times 0.586 \times 1 \text{ mm}^3$	
UFH01MF	2 year F $0.379 \times 0.379 \times 4.5 \text{ mm}^3$	1 year F $0.406 \times 0.406 \times 3 \text{ mm}^3$		
UFH05MF		4 year F $0.451 \times 0.451 \times 5 \text{ mm}^3$		
UFH10MF	12 year M $0.469 \times 0.469 \times 6 \text{ mm}^3$	11 year M $0.469 \times 0.469 \times 6 \text{ mm}^3$		
UFH15M	18 year M ^a 1 mm	14 year M $0.625 \times 0.625 \times 6 \text{ mm}^3$	15 year F $0.21 \times 0.21 \times 0.75 \text{ mm}^3$	18 year M ^c 1 mm
UFH15F	15 year F $0.449 \times 0.449 \times 4.5 \text{ mm}^3$	14 year F $0.742 \times 0.742 \times 6 \text{ mm}^3$	(all ages except newborn)	(all ages except newborn)
UFHADM	18 year M 1 mm	36 year M $1.97 \times 1.97 \times 3 \text{ mm}^3$		
UFHADF	15 year F ^b $0.449 \times 0.449 \times 4.5 \text{ mm}^3$	25 year F $0.66 \times 0.66 \times 5 \text{ mm}^3$		

^a Head model of UFHADM was downscaled to create the UFH15M head model.

^b Head model of UFH15F was upscaled to create the UFHADF head model.

^c High resolution (1 mm slice thickness) CT images of arms and legs were obtained from an 18 year male cadaver.

ICRP Modifications of the UF/NCI Hybrid Phantoms

- *Additional organs and tissues to match those in the ICRP 110 adult phantom*
 - *Breast tissues, blood vessels in the lungs, ureters, etc.*
- *Generation of a lymphatic node model*
- *Construction of new models of adipose tissue and skeletal muscle*
- *Re-tagging tissue regions to again match ICRP 110 tag list*

Phantom	Voxel Resolution (cm)			Number of Voxels			Total Matrix Size ($\times 10^6$)
	X-direction	Y-direction	Z-direction	X-direction	Y-direction	Z-direction	
UFH00MF	0.0663	0.0663	0.0663	350	215	720	54.18
UFH01MF	0.0663	0.0663	0.1400	396	253	550	55.10
UFH05MF	0.0850	0.0850	0.1928	416	235	576	56.31
UFH10MF	0.0990	0.0990	0.2425	428	226	580	56.10
UFH15M	0.1250	0.1250	0.2832	414	226	590	55.20
UFH15F	0.1200	0.1200	0.2828	410	238	574	56.01
ICRP AF	0.1775	0.1775	0.484	299	137	348	14.26
ICRP AM	0.2137	0.2137	0.8000	254	127	222	7.16

Presentation Objectives

- 1. Review current work flow of ICRP Committee 2 and its Task Groups**
 - A. Dose coefficients for adult phantoms
 - B. Dose coefficients for pediatric phantoms
- 2. Review the historical lineage of models that have become the ICRP pediatric phantom series**
- 3. Review specific dosimetry models associated with these pediatric phantoms**
 - A. Blood distribution
 - B. Skeletal tissue models
 - C. SAFs for internally emitted radiations
- 4. Review the development and two specific applications of a derived pediatric phantom library**
 - A. Radiation epidemiology of the medical imaging of children
 - B. Radiation epidemiology of the Japanese atomic bomb survivors

Pediatric Blood Distribution Model

Table 1. Reference values for total blood volume (cm³).

Age	Male	Female
Newborn	270	270
1-year	500	500
5-year	1400	1400
10-year	2400	2400
15-year	4500	3300
Adult	5300	3900

Source: ICRP Publication 89, Section 7.4

Table 2. Reference values for relative regional blood volumes in the reference adults.

Organ or Tissue	Blood Content (% Total Blood Volume)	
	Adult Male	Adult Female
Fat	5.00	8.50
Brain	1.20	1.20
Stomach & Esophagus Wall	1.00	1.00
Small Intestine Wall	3.80	3.80
Large Intestine Wall	2.20	2.20
Right Heart Contents	4.5	4.50
Left Heart Contents	4.5	4.50
Coronary Tissues	1.00	1.00
Kidneys	2.00	2.00
Liver	10.00	10.00
Pulmonary Tissues	10.50	10.50
Bronchial Tissues	2.00	2.00
Skeletal Muscle	14.00	10.50
Pancreas	0.60	0.60
Skeletal Tissues		
Active Marrow	4.00	4.00
Trabecular Bone	1.20	1.20
Cortical Bone	0.80	0.80
Miscellaneous Skeletal Tissues	1.00	1.00
Skin	3.00	3.00
Spleen	1.40	1.40
Thyroid	0.06	0.06
Lymphatic Nodes	0.20	0.20
Testes or Ovaries	0.04	0.02
Adrenal Glands	0.06	0.06
Urinary Bladder Wall	0.02	0.02
All Other Tissues	1.92	1.92
Aorta and Large Arteries	6.00	6.00
Large Veins	18.00	18.00
	100.00	99.98

Source: ICRP Publication 89, Section 7.7.2

Pediatric Blood Distribution Model

Table 3. Vascular scaling factors for tissues with changing rates of blood vessel growth.

Age	Brain	Trabecular		Cortical
		Kidneys	Bone	Bone
Newborn	1.04	0.67	4.70	2.60
1-year-old	1.16	0.67	4.70	2.60
5-year-old	1.39	1.00	4.40	2.40
10-year-old	1.33	1.00	4.00	2.20
15-year-old	1.13	1.00	3.70	1.90
Adult	1.00	1.00	1.00	1.00

$$f_{blood}^{organ}(a, s) = \frac{V_{blood}^{organ}(adult, s)}{\sum V_{blood}^{organ}(adult, s)}$$

$$V_{blood}^{organ}(a, s) = R_{vas}^{organ}(a, s) \times V_{blood}^{organ}(adult, s) \times \left[\frac{V_{parenchyma}^{organ}(a, s)}{V_{parenchyma}^{organ}(adult, s)} \right]$$

Pediatric Skeletal Tissue Models

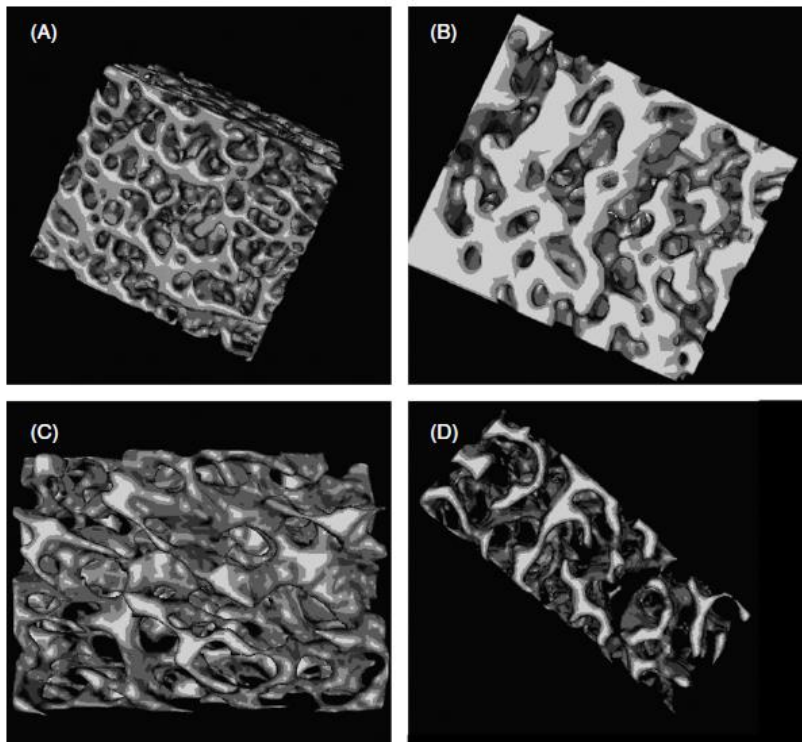


Figure 4. Spongiosa sections of 3D-rendered image threshold marrow and trabecular bone for (A) 4 day old L₃, (B) 4 day old sternum, (C) 5 day old fourth rib and (D) 5 day old iliac crests.

Phys. Med. Biol. 54 (2009) 4497–4531

An image-based skeletal tissue model for the ICRP reference newborn

Deanna Pafundi¹, Choonsik Lee¹, Christopher Watchman²,
Vincent Bourke², John Aris³, Natalia Shagina⁴, John Harrison⁵, Tim Fell⁵
and Wesley Bolch^{1,6}

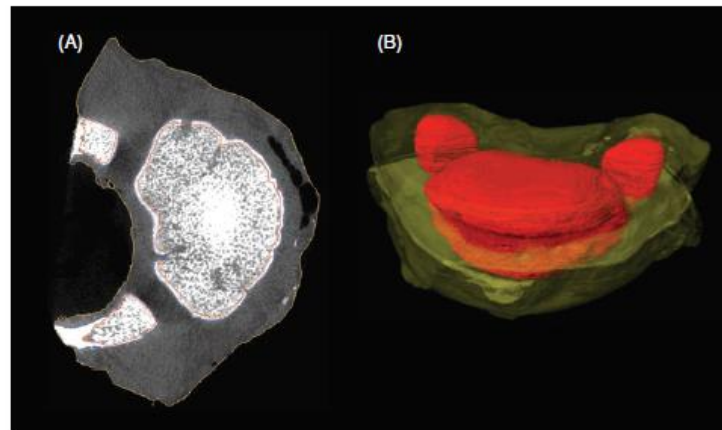
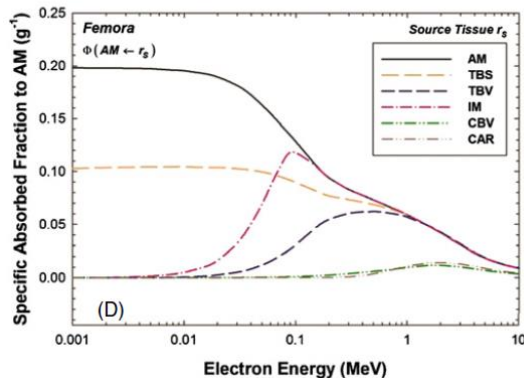
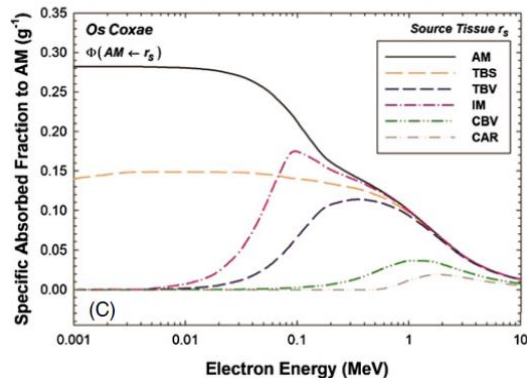
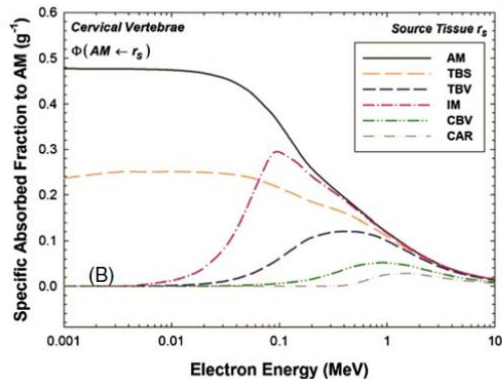
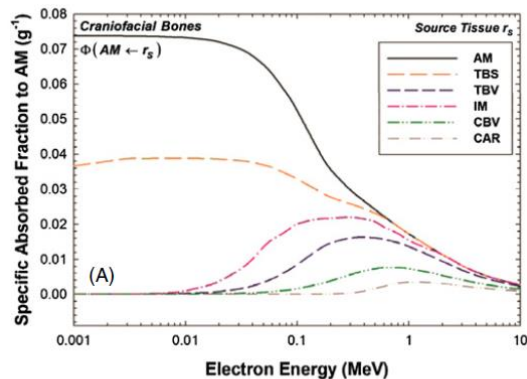


Figure 3. (A) Segmented transverse slice of 4 day old L₃ using 3D-Doctor and (B) 3D rendering of segmented 4 day old L₃ using 3D-Doctor.

Pediatric Skeletal Electron and Photon Dosimetry Models



Phys. Med. Biol. 55 (2010) 1785–1814

An image-based skeletal dosimetry model for the ICRP reference newborn—internal electron sources

Deanna Pafundi¹, Didier Rajon², Derek Jokisch³, Choonsik Lee¹
 and Wesley Bolch^{1,4,5}

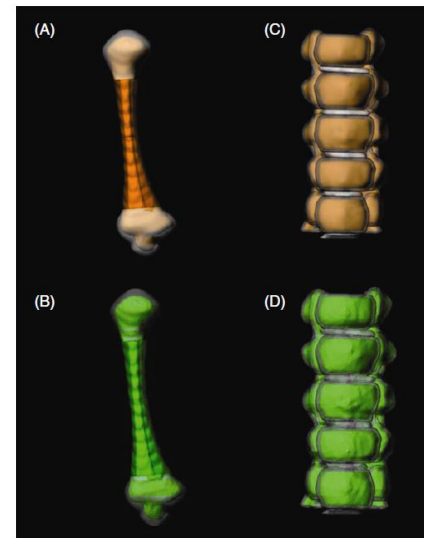


Figure 1. Rendered images of the original polygon mesh and segmented voxelized newborn skeletal models: (A) polygon mesh model of the femur, (B) voxelized model of the femur, (C) polygon mesh model of the lumbar vertebrae and (D) voxelized model of the lumbar vertebrae.

Pediatric SAFs – Photons, Electrons, Alpha Particles, Fission Neutrons

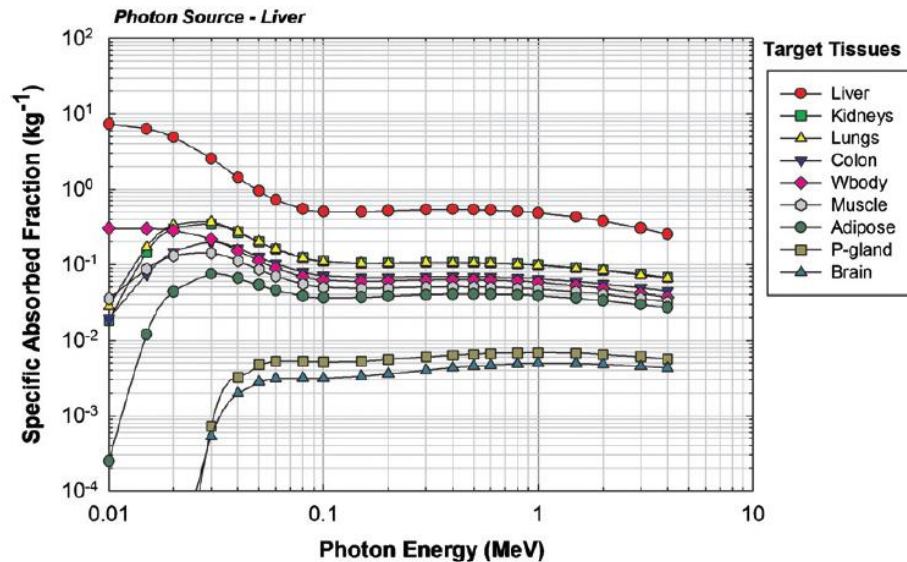


Figure 5. Photon SAFs for a uniform photon source in the newborn liver. Target organs are given in the legend in decreasing order of their SAF at 4 MeV.

Phys. Med. Biol. **57** (2012) 1433–1457

Internal photon and electron dosimetry of the newborn patient—a hybrid computational phantom study

Michael Wayson¹, Choonsik Lee², George Sgouros³, S Ted Treves⁴,
Eric Frey³ and Wesley E Bolch^{1,5}

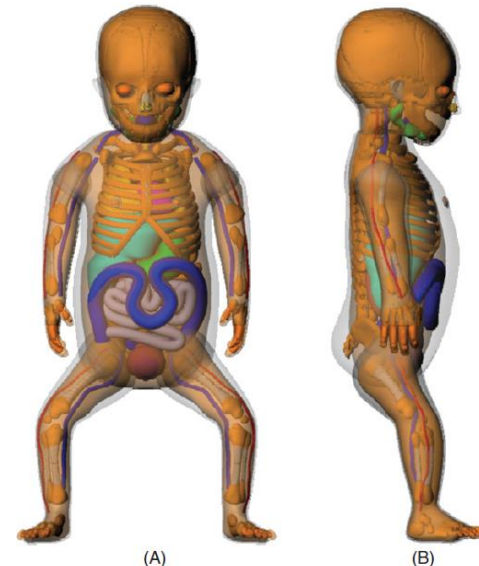
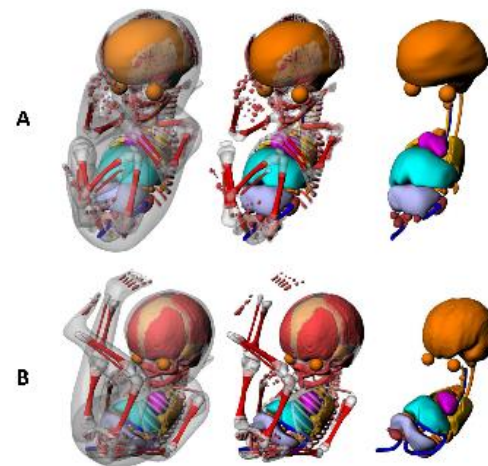
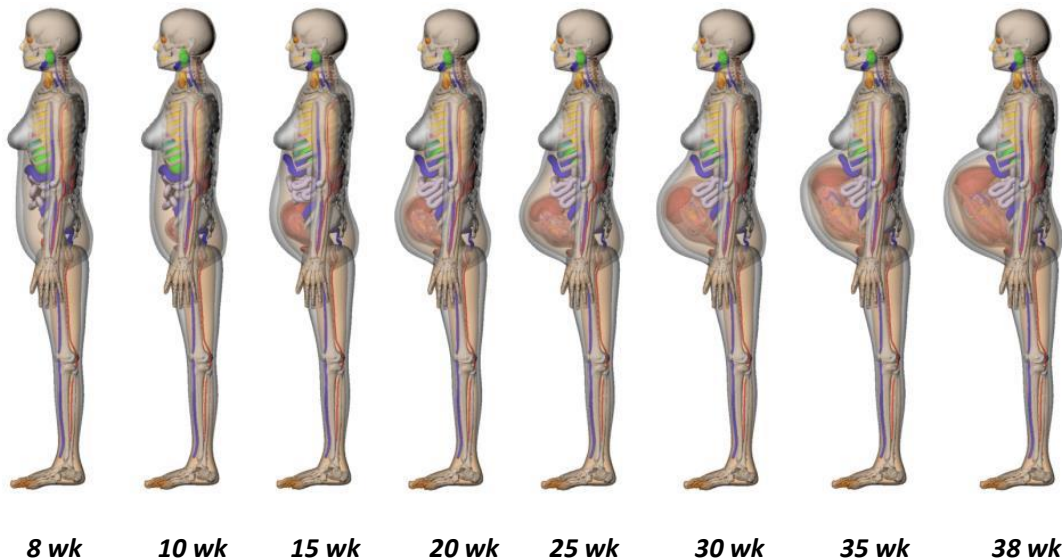


Figure 1. (A) Front and (B) side 3D views of the UF hybrid-NURBS/PM newborn female phantom.

UF/NCI Phantom Library – Pregnant Females



The UF Family of hybrid phantoms of the pregnant female for computational radiation dosimetry

Phys. Med. Biol. **59** (2014) 4325–4343

Matthew R Maynard¹, Nelia S Long¹, Nash S Moawad²,
Roger Y Shifrin³, Amy M Geyer¹, Grant Fong⁴ and
Wesley E Bolch^{1,5}

The UF family of hybrid phantoms of the developing human fetus for computational radiation dosimetry

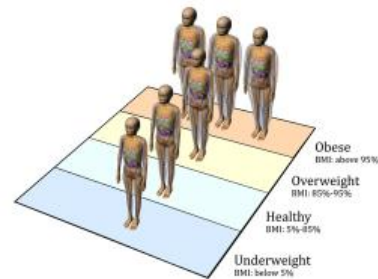
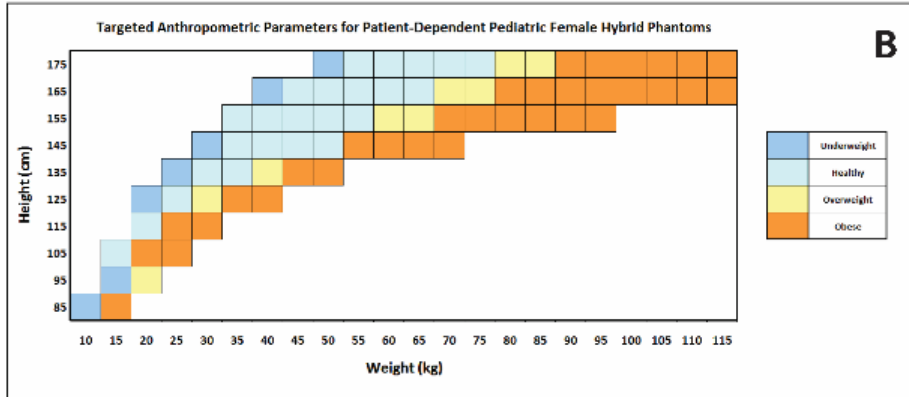
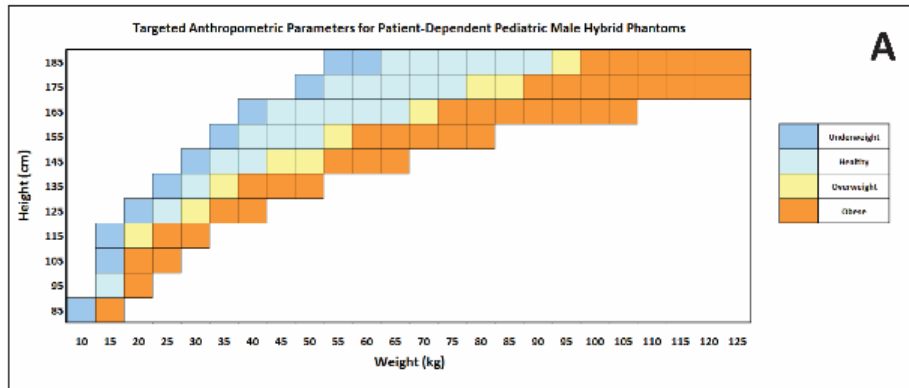
Phys. Med. Biol. **56** (2011) 4839–4879

Matthew R Maynard¹, John W Geyer¹, John P Aris², Roger Y Shifrin³
and Wesley Bolch^{1,4,5}

Presentation Objectives

- 1. Review current work flow of ICRP Committee 2 and its Task Groups**
 - A. Dose coefficients for adult phantoms
 - B. Dose coefficients for pediatric phantoms
- 2. Review the historical lineage of models that have become the ICRP pediatric phantom series**
- 3. Review specific dosimetry models associated with these pediatric phantoms**
 - A. Blood distribution
 - B. Skeletal tissue models
 - C. SAFs for internally emitted radiations
- 4. Review the development and two specific applications of a derived pediatric phantom library**
 - A. Radiation epidemiology of the medical imaging of children
 - B. Radiation epidemiology of the Japanese atomic bomb survivors

UF/NCI Phantom Library - Children



Phantom for each height/weight combination further matching average values of body circumference from CDC survey data

*85 pediatric males
73 pediatric females*

The UF family of reference hybrid phantoms for computational radiation dosimetry

Phys. Med. Biol. 55 (2010) 339–363

Choonsik Lee¹, Daniel Lodwick², Jorge Hurtado², Deanna Pafundi², Jonathan L Williams³ and Wesley E Bolch^{4,5}

The UF/NCI family of hybrid computational phantoms representing the current US population of male and female children, adolescents, and adults—application to CT dosimetry

Phys. Med. Biol. 59 (2014) 5225–5242

Amy M Geyer¹, Shannon O'Reilly¹, Choonsik Lee², Daniel J Long¹ and Wesley E Bolch¹

UF/NCI Phantom Library - Children

Table 1. Mapping of reference phantoms and direction of height scaling performed to create the initial set of anchor phantoms by height for the various four patient-dependent libraries.

Phantom height (cm)	Pediatric		Phantom height (cm)	Adult	
	Males	Females		Males	Females
185	UFHADM ↑		190	UFHADM ↑	
175	UFHADM ↓	UFHADF ↑	185	UFHADM ↑	
165	UFH15M ↓	UFHADF ↑	180	UFHADM ↑	
155	UFH15M ↓	UFH15F ↓	175	UFHADM ↓	UFHADF ↑
145	UFH10M ↑	UFH10F ↑	170	UFH15M ↑	UFHADF ↑
135	UFH10M ↓	UFH10F ↓	165	UFH15M ↓	UFHADF ↑
125	UFH10M ↓	UFH10F ↓	160	UFH15M ↓	UFH15F ↓
115	UFH05M ↑	UFH05F ↑	155		UFH15F ↓
105	UFH05M ↓	UFH05F ↓	150		UFH15F ↓
95	UFH05M ↓	UFH05F ↓			
85	UFH01M ↑	UFH01F ↑			

The naming convention for the UF phantom series begins with the identifier UFH (University of Florida Hybrid), followed by the reference phantom age in years (00, 01, 05, 10, 15 and AD for adult) and then the phantom gender (M for male and F for female).

The UF/NCI family of hybrid computational phantoms representing the current US population of male and female children, adolescents, and adults—application to CT dosimetry

Phys. Med. Biol. 59 (2014) 5225–5242

Amy M Geyer¹, Shannon O'Reilly¹, Choonsik Lee²,
Daniel J Long¹ and Wesley E Bolch¹

Risk of Pediatric and Adolescent Cancer Associated with Medical Imaging

R01 CA185687

The use of medical imaging that delivers ionizing radiation is high in the United States. The potential harmful effects of this imaging must be understood so they can be weighed against its diagnostic benefits, and this is especially critical for our vulnerable populations of children and pregnant women. The proposed study will comprehensively evaluate patterns of medical imaging, cumulative exposure to radiation, and subsequent risk of pediatric cancers in four integrated health care delivery systems comprising over 7 million enrolled patients enrolled from 1996-2017.

Project Management

University of California, San Francisco (UCSF)

Biostatistics and Epidemiology

University of California, Davis (UCD)

Organ Dose Assessment

University of Florida (UF)

Patient Enrollment Sites

Kaiser Permanente Northern California (KPNC)

Kaiser Permanente North West (KPNW)

Kaiser Permanente Hawaii (KPHI)

Kaiser Permanente Washington (KPWA)

Marshfield Clinic Research Institute (MCRI)

Pediatric Oncology Group of Ontario (POGO)

Geisinger Health Systems (GE)

Harvard Pilgrim Health Plan (HP)

Risk of Pediatric and Adolescent Cancer Associated with Medical Imaging

R01 CA185687

Aim 1: Imaging Utilization Patterns

Aim 1A – Patterns of imaging utilization in pregnant women

Aim 1B – Patterns of imaging utilization in children

Aim 1C – Patterns of imaging utilization in adults and children

Aim 2: Organ Dose and Association with Cancer Outcomes

Aim 2A – Imaging in pregnant women and childhood cancer risk

Aim 2B – Imaging in children and childhood leukemia risk

Aim 2C – Imaging in pregnant women and children and childhood cancer risk

1. Organ Dose Reconstruction in Computed Tomography

Data Collection – 2006 to 2017

Data Collection – 1996 to 2006

Radimetrics

Data Abstraction

Patient Data

Study ID

Age

Gender

Height

Weight

Effective diameter at center slice (cm)

Pregnant Females

Gestational age

CT Procedure Details

Year of scan

Scan # in current year

Series # in current scan

Body part imaged

Medical facility

CT scanner manufacturer

CT scanner model

CT Technique Factors

Scan length (cm)

Beam collimation (mm)

Beam energy (kVp)

Pitch

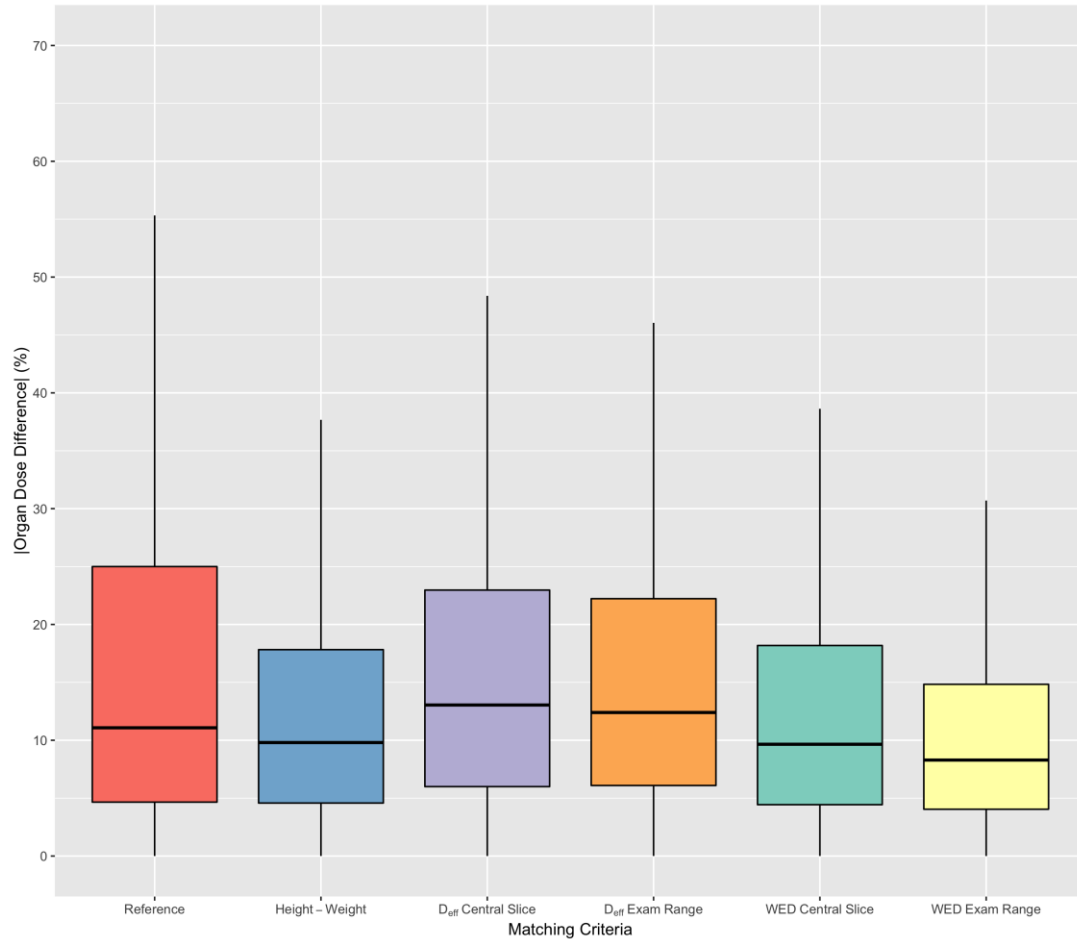
CTDIvol (mGy)

DLP (mGy-cm)

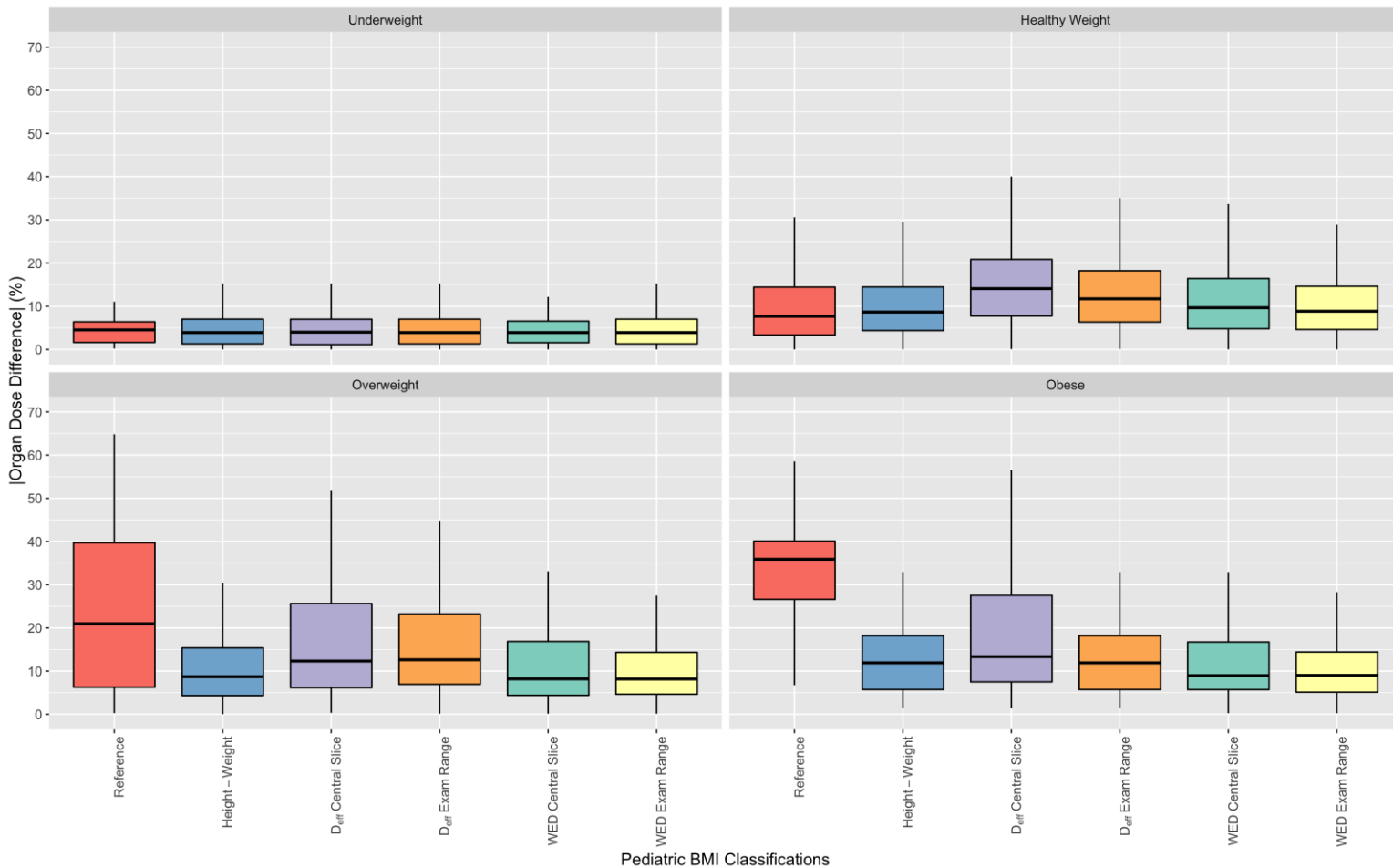
Fixed or modulated mA

Exam Averaged mAs

Boxplots comparing all organ dose percent differences for each of the six matching parameters. The vertical lines extend at most 1.5 times the interquartile.



Boxplots comparing organ dose percent difference for each of the six matching parameters based on CDC BMI classifications for pediatric patients. The vertical lines extend at most 1.5 times the interquartile range.



2. Organ Dose Reconstruction in Diagnostic Fluoroscopy

Data Collection – 2006 to 2017

Data Collection – 1996 to 2006

Radimetrics

Data Abstraction

Patient Data

Study ID
Age
Gender
Height
Weight

Fluoroscopy Procedure Details

Procedure type (1 to 6)
Cumulative fluoroscopy time
Cumulative reference air kerma
Cumulative kerma-area product

Reference Fluoroscopy Exams

1. Upper Gastrointestinal Series (UGI)
2. Upper Gastrointestinal Series with Follow-Through (UGI-FT)
3. Voiding Cystourethrogram (VCUG)
4. Rehabilitation Swallow (RS)
5. Lower Gastrointestinal Series / Barium Enema (LGI)
6. Gastrostomy Tube Placement (G-Tube)

Problem – nearly all diagnostic fluoroscopy systems cannot generate RDSRs

Solution – create “reference” diagnostic exams and scale doses by FT, RAK, KAP

3. Organ Dose Reconstruction in Diagnostic Nuclear Medicine

Data Collection – 2006 to 2017

Data Collection – 1996 to 2006

Radimetrics

Data Abstraction

Patient Data

Study ID

Age

Gender

Height

Weight

NM Procedure Details

Procedure type (1 to 6)

Administered Activity

Reference NM Procedures

1. *Tc-99m DMSA*

2. *Tc-99m MDP*

3. *Tc-99m MAG3*

4. *F-18 FDG*

5. *TBD*

6. *TBD*

Problem – *Injected activity might not be available*

Solution – *Use current guidelines or period-specific weight-based dosing schemes*

Biokinetics – *Assume ICRP TG36 reference models*

Radionuclide S values – *Assume values from the UF reference phantoms*

Radiation Effects Research Foundation (RERF) Pilot Study

Reassess the Organ Dosimetry of the Atomic Bomb Survivors in Hiroshima and Nagasaki

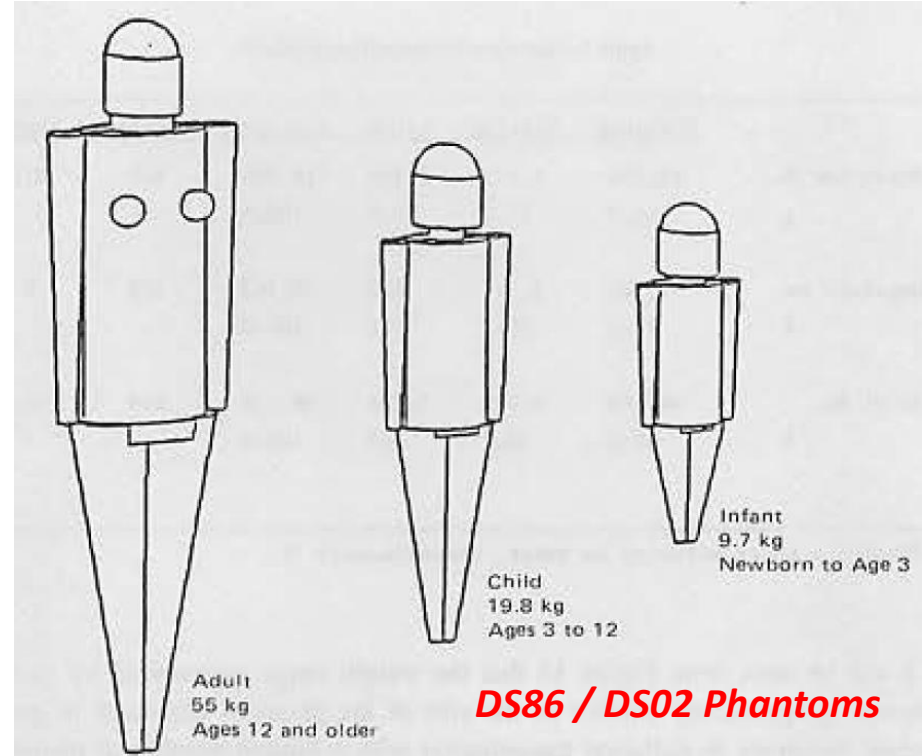
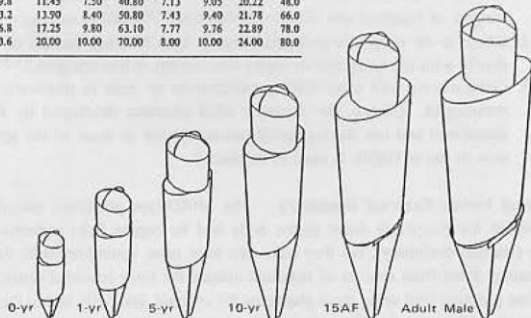
Major Dosimetry Systems from RERF:

TD65 – Mostly experimentally based

DS86 – Monte Carlo based

DS02 – Update to DS86

Phantom	Weight (kg)	A_T (cm)	B_T (cm)	C_T (cm)	A_M (cm)	B_M (cm)	C_M (cm)	C_L (cm)
0-yr	3.6	6.35	4.90	21.60	4.52	5.78	13.09	16.8
1-yr	9.7	8.80	6.50	30.70	6.13	7.84	17.76	26.5
5-yr	19.8	11.45	7.50	40.80	7.13	9.05	20.22	48.0
10-yr	33.2	13.90	8.40	50.80	7.43	9.40	21.78	66.0
15AF	56.8	17.25	9.80	63.10	7.77	9.76	22.89	78.0
Adult male	73.6	20.00	10.00	70.00	8.00	10.00	24.00	80.0



Radiation Effects Research Foundation (RERF) Pilot Study

Reassess the Organ Dosimetry of the Atomic Bomb Survivors in Hiroshima and Nagasaki

Table 1. Average Weight of Organs for the Normal Japanese Adult as Compared with the Data of the ICRP

Organs	Male			Female		
	Japanese			Japanese		
	Tanaka (1979)	Aimi (1952)	ICRP (1975)	Tanaka (1979)	Aimi (1952)	ICRP (1975)
Adrenal glands	14.7g	11.1g	13.8g	13.2g	10.5g	12.7g
Brain	1,440	1,424	1,355	1,308	1,256	1,220
Heart	352	309	330	284	249	240
Kidneys	327	269	310	280	235	275
Liver	1,600	1,431	1,831	1,363	1,269	1,477
Lungs	1,162		1,169	893		
Pancreas	135		96.1	111		84.8
Pituitary gland	0.56	0.66	0.55	0.63	0.75	0.62
Spleen	127	109	192	122	106	153
Testes	35.3		34.7			
Thymus	31.7	24.9	19.7	25.6	21.7	19.7
Thyroid	19.1	18.8	17.6	16.8	17.2	14.5

Tanaka et al.²¹

Aimi et al.²²

ICRP Publication 25.²³

Radiation Effects Research Foundation (RERF) Pilot Study

Reassess the Organ Dosimetry of the Atomic Bomb Survivors in Hiroshima and Nagasaki

Table 4. Standard Japanese Phantom Specifications by Age and Sex

Age	0	1	5	10	15	20	
						Male	Female
Height (cm)	49	74	102	126	150	162	152
Weight (kg)	2.8	8.5	16	25.5	44	54	50
Circumference of the chest	32	46	54	61	63	83	81
Length of trunk, neck and head	32	46	59	70	82	88	84

New RERF phantom series will include newborn to adults (male and female) and pregnant female phantoms at 3-5 stages of gestation (standing, lying, kneeling)

Thank you for your attention!

